Proceedings of the
International Conference on Mechanical Engineering 2005
(ICME2005) 28- 30 December 2005, Dhaka, Bangladesh

ICME05-FL-10

FLOW MEASUREMENTS IN THE A-PILLAR REGIONS OF A SERIES IDEALISED PASSENGER CARS

Firoz Alam[1], **Simon Watkins**[1] **and Gary Zimmer**[2]

[1]School of Aerospace, Mechanical and Manufacturing Engineering, RMIT University
264 Plenty Road, Bundoora, Melbourne, VIC 3083, Australia
[2]School of Science and Engineering, Ballarat University, Ballarat, VIC 3353, Australia

ABSTRACT

The air flow around the A-pillar regions of a passenger car is a primary source of aerodynamic noise. Aerodynamically induced noise adversely affects passenger comfort and safety. High aerodynamic noise levels can not only make it difficult for vehicle occupants to converse or listen to the radio but also cause driver fatigue on a long highway trip. Many modern cars still have high fluctuating exterior hydrodynamic pressure due to flow separation in the A-pillar region. The size and magnitude of the A-pillar flow separation mainly depend on the local A-pillar and windshield geometry and yaw angles. Therefore, as a part of a larger study, the primary objective of this work was to measure the mean and fluctuating pressures of a series idealised road vehicles. The surface mean and fluctuating pressures were measured using Dynamic Pressure Measuring Systems in the RMIT Industrial Wind Tunnel under a range of speeds and yaw angles. Air flow structure was visualised with smoke and wool tufts.

Keywords: Surface Mean Pressure, Fluctuating Pressure, Wind Tunnel, Wind Noise.

1. INTRODUCTION

The air flow around the A-pillar regions of a passenger car is a primary source of aerodynamic noise as strong flow separation occurs here due to complex A-pillar geometry (see [1], [2], [3], [4], [5] and [6]. A-pillar of a car can be defined as the structural joint between the windshield and front side window. Aerodynamic noise adversely affects occupant's comfort as other sources of noise (e.g., engine, transmission and road/tyre interaction noise) are less dominant at high speeds (100 km/h and over). High aerodynamic noise levels can not only make it difficult for vehicle occupants to converse or listen to the radio but also cause driver fatigue on a long highway trip. Due to the flow separation in the A-pillar region, a rotational vortex is formed in the A-pillar region and it expands and travels towards the roof. This conical vortex generates not only acoustic waves but also causes side window to vibrate and radiate noise into the interior of the vehicle. Many modern cars still have high fluctuating exterior hydrodynamic pressure due to flow separation in the A-pillar region. The size and magnitude of the A-pillar flow separation mainly depend on the local A-pillar and windshield geometry and yaw angles. The primary objectives of this work are to investigate the effects of A-pillar geometry on the potential for noise generation of production vehicles. For this purpose, three simplified 40% scale models and one 30% scale model (correct replica) of a production family size passenger car were used to measure the surface mean and fluctuating pressures around the side window in the A-pillar region and to see how the magnitude of the pressure varies with A-pillar radii. Testing was conducted in the RMIT University Industrial Wind Tunnel. A plan view of the RMIT Industrial Wind Tunnel is shown in Figure 1. Flow structure around the A-pillar region was documented using flow visualization.

2. MODEL DESCRIPTION, TEST PROCEDURE AND DATA PROCESSING

In order to study the effects of A-pillar and windshield geometry on the local flow (e.g., mean and fluctuating pressures), three 40% scale idealised vehicles (models) with different A-pillar and windshield geometry were made. A 30% scale model of a production passenger car was also used. The 40% scale model was a compromise between minimising the blockage ratio and obtaining as close to full-size Reynolds number as possible. These models were kept simple without the added complication of wheels, wheel arches, engine compartment flow, side mirrors and fore-body details. In addition, models had no ground clearance and were parallel-sided in plan view. However, the 30% scale model was a correct replica of a production vehicle with wheels, wheel arches, engine compartment flow, side mirrors and fore-body details. The variables were the A-pillar/windshield curvature, Reynolds number (varied by tunnel speed) and yaw angle. Each of the four models has different A-pillar/windshield

curvatures (100R, 200R and 299R and replica close to 100R) all with 60° windshield inclination angles. A typical simplified scale model and Ford model are shown in Figures 2, 3, 5 and 6 respectively.

As mentioned earlier, tests were performed in the RMIT University Industrial Wind-Tunnel. The surface mean and fluctuating pressures were measured at speeds of 60, 80, 100, 120 and 130 km/h under different yaw angles (0 and ±15°) for all models. In order to obtain a comprehensive pressure distribution, 60 pressure holes were drilled normal to the window surface in three rows for each of the model's front side window. The bottom row was approximately 1/4 distance away from the baseline of the window, the middle row was 2/4 and the top row was 3/4 the distance from the window base. The diameter of the hole was 2 mm. The space between the two holes was 25 mm horizontally. Before drilling the holes, flow visualisation was carried out to determine flow in the area of interest (i.e., the region that is influenced by the A-pillar vortex). Each hole was pressure tapped with rubber tubing that was connected to four pressure sensor modules of Dynamic Pressure Measurement System (DPMS) and later to Interference box which was connected to a data acquisition system (a dedicated computer). Figure 4 shows the pressure modules and the interference box. The DPMS data acquisition software provides mean (time averaged), rms (time dependent fluctuating), minimum and maximum pressure values of each pressure port. For the given tubing dimensions (length and diameter), the data can be linearised to correct for the tubing response in order to obtain accurate dynamic pressure measurements. The sampling frequency of each channel was 1250 Hz. It may be noted that the peak energy of fluctuating pressure on window surface in the A-pillar region is well below 500 Hz, [1].

The time-averaged and time fluctuating pressure distributions were then converted to the non-dimensional pressure coefficients (Cp) and Cp rms using the following relation:

$$C_p = \frac{p_m - p_\infty}{\frac{1}{2}\rho V_\infty^2} \text{ and } C_{p\,rms} = \frac{p_{std}}{\frac{1}{2}\rho V^2} \text{ respectively.}$$

Here p_m is the time-averaged surface pressure on the side window near the A-pillar), p_∞ is the free stream static pressure, V_∞ is the free stream, p_{std} is the standard deviation of the fluctuating pressure and $\frac{1}{2}\rho V^2$ is the mean velocity head (q). The mean velocity head was obtained from the tunnel data acquisition system.

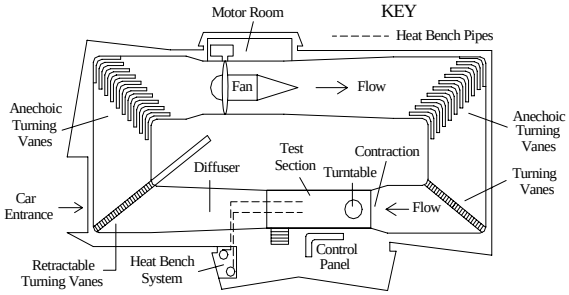

Fig 1. A plan view of RMIT Industrial Wind Tunnel

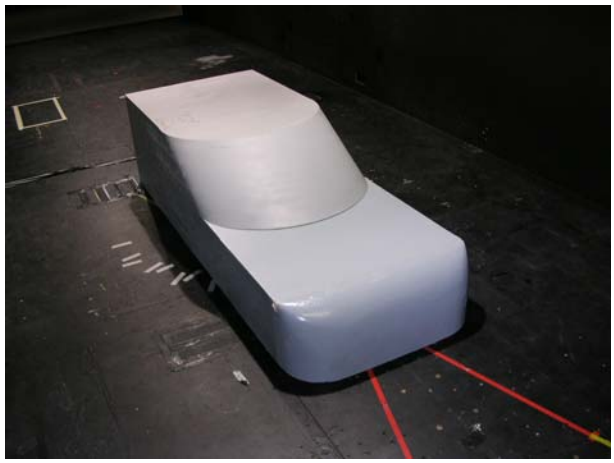

Fig 2. A typical simplified model in the test section

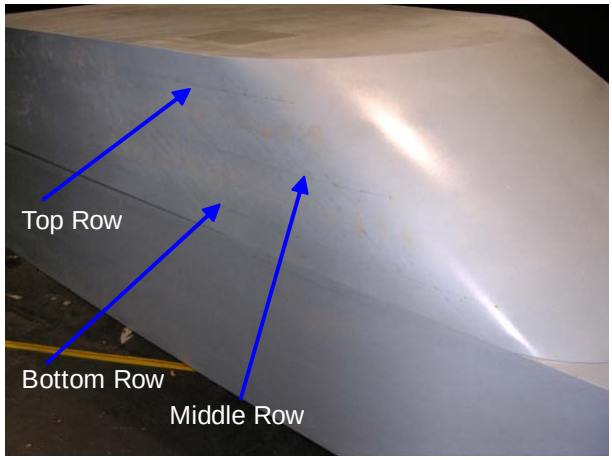

Fig 3. A-pillar region of a simplified model

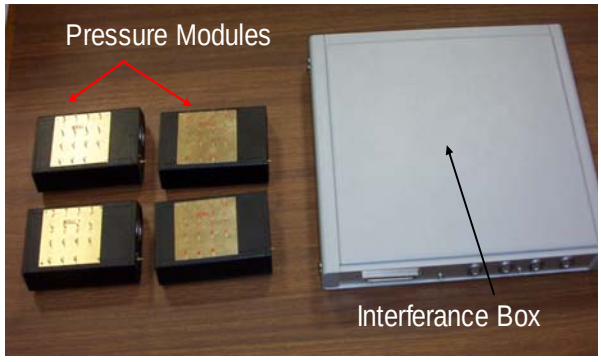

Fig 4. Components of DPMS

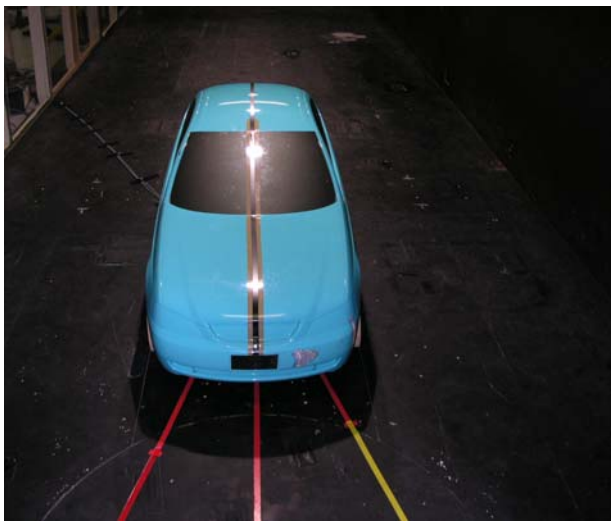

Fig 5. Ford scale model in the test section

Fig 6. Ford scale model with side view

3. RESULTS AND DISCUSSION

As mentioned earlier, the surface mean and fluctuating pressures were converted to non dimensional surface mean pressure coefficient (Cp) and fluctuating pressure coefficient (Cp rms). The surface mean and fluctuating pressure coefficients for the Ford model and 100R simplified model have been plotted against the distance from the line of symmetry (at the front) of the models (for details of how the graphical results relate to the model geometry, refer to [1]. The mean Cp and fluctuating Cp rms are shown in 2D and 3D in Figures 7 to 26. Figures 7, 9, 17 and 19 show the mirror image of the mean and fluctuating pressure distributions to the left and right hand sides of the Ford model and simplified model (100R). Figures 11, 14 , 21 and 24 show the Cp and Cp rms for -15 yaw angle (left hand side) and +15 Yaw angle (right hand side) in the same plot. The results for other models were not presented in this work.

The magnitude of the mean and fluctuating pressure coefficients is shown in grid pattern in 3D plots (see Figures 8, 10, 12,13, 15, 16, 18, 20, 22, 23, 25 and 26) for zero and ±15º yaw angles respectively. The Cp and Cp rms (except 3D plots) are shown for the bottom, middle and top rows along the side window in the A-pillar region. Figures 7, 9 and 11 indicate that the mean Cp and fluctuating Cp rms for the Ford model are relatively independent of Reynolds numbers for zero yaw angles and ±15º yaw angles. However, a small variation in Cp rms at -15º yaw angles is noted (see Figure 14). A similar trend for the simplified model is also evident (see Figures 17, 19, 21 and 24). However, a significant Reynolds number dependency is noted at -15º yaw angles for the simplified model (100R). The simplified model has the tighter A-pillar and windshield radius than the Ford model. Due to the tighter radius, the 100R model (simplified) generates stronger flow separation in the A-pillar region than the Ford model. The simplified model has the higher magnitudes of Cp and Cp rms values at all yaw angles compared to the Ford model. Generally, the magnitude of the fluctuating pressure is much smaller at the windward (positive) side yaw angles compared to the leeward (negative) yaw angles which is evident for the Ford model (see Figure14). However, it is not the case for the simplified model. A further investigation is required to clarify this phenomenon.

The magnitude of surface mean and fluctuating pressure distributions in 3D are shown in Figures 8, 10, 12, 13, 15, 16, 18, 20, 22, 23, 25 & 26. Figures show the formation of a strong conical vortex on the side window along the A-pillar edge that expands and travels towards the roof. The pattern of surface mean pressure for the simplified model and the Ford model (correct replica) looks very similar but slightly different in magnitude as expected due to variation of detailed geometry. The plots of surface fluctuating pressure coefficients for both scale models show a very good correlation except the positive yaw angles for the simplified model. However, the surface mean pressure coefficient (Cp) does not correlate well. A further investigation is underway to clarify the discrepancy. It may be noted that the Ford model has a very complex A-pillar radius and angle which were not produced in the simplified model as mentioned earlier. The purpose of the selection of these two models is to compare the results with each other as the simplified model's local A-pillar and windshield geometry are severely compromised.

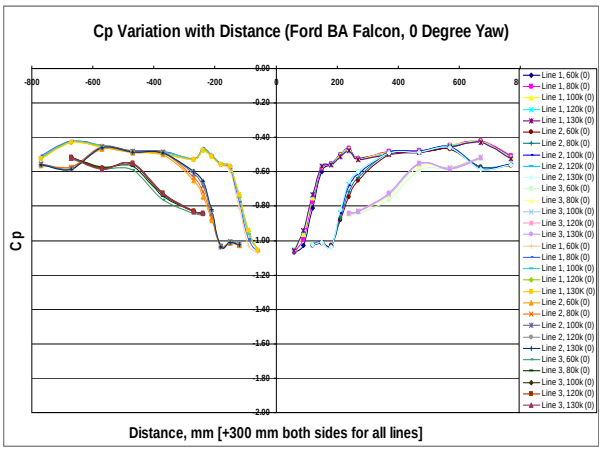

Fig 7. Mean Cp Variation, 0 Yaw angle, Ford Model

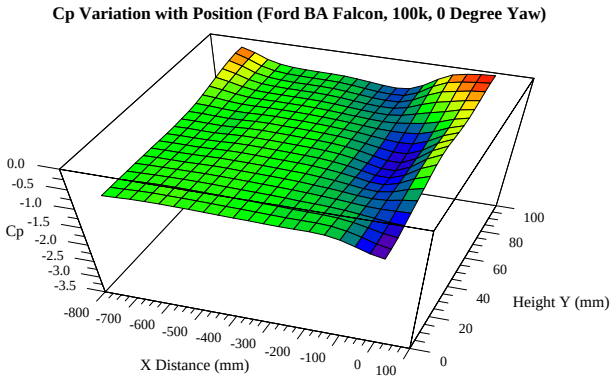

Fig 8. Mean Cp Variation, 0 Yaw angle, Ford Model

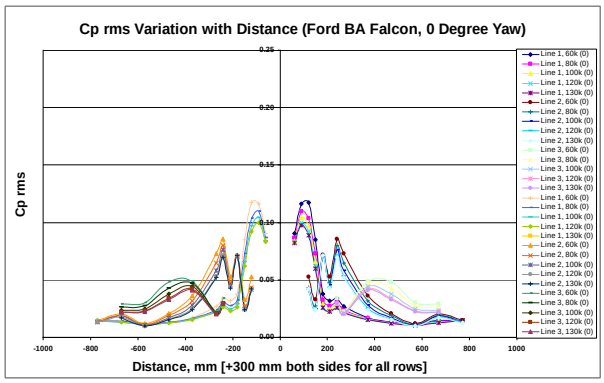

Fig 9. Fluctuating Cp rms Variation, 0 Yaw angle, Ford Model

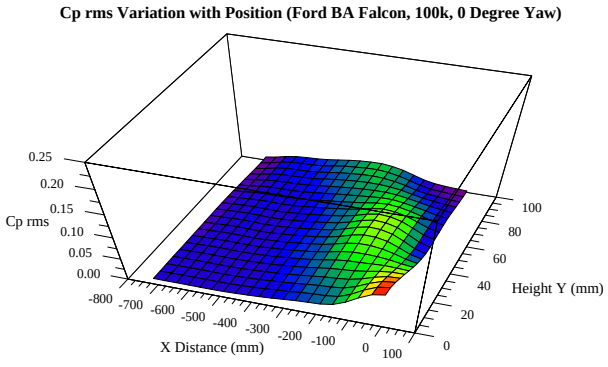

Fig 10. Fluctuating Cp rms Variation, 0 Yaw angle, Ford Model

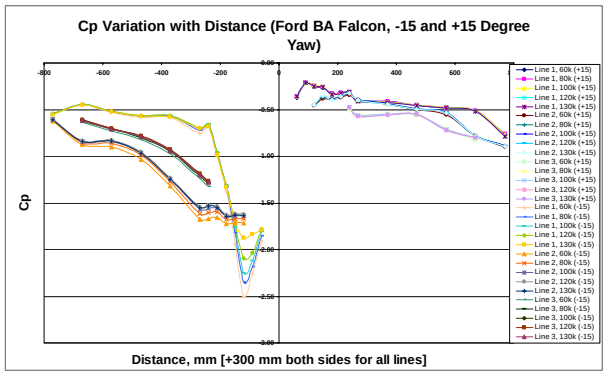

Fig 11. Mean Cp Variation, ±15º Yaw angles, Ford Model

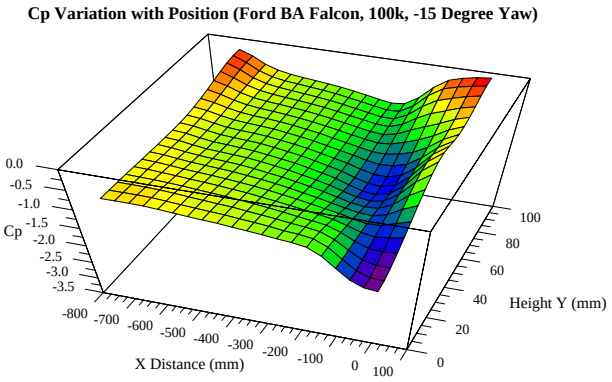

Fig 12. Mean Cp Variation, -15º Yaw angles, Ford Model

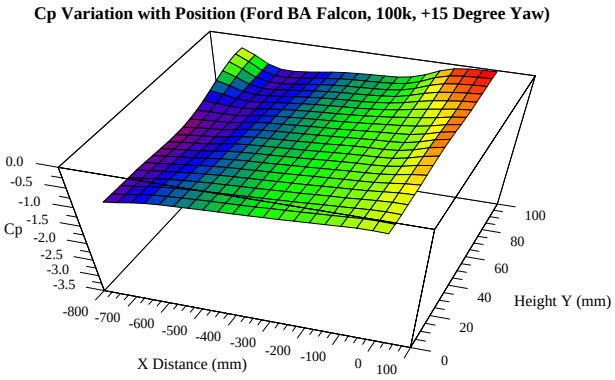

Fig 13. Mean Cp Variation, +15º Yaw angles, Ford Model

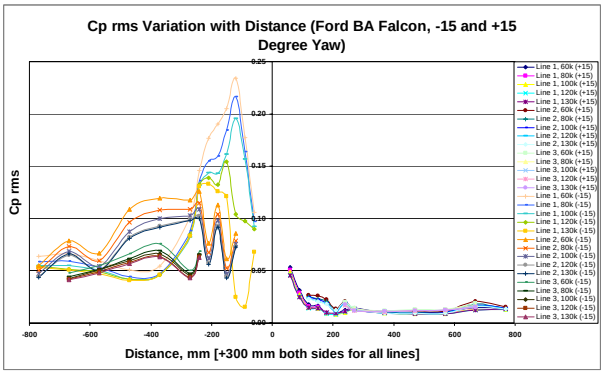

Fig 14. Fluctuating Cp rms Variation, ±15º Yaw angles, Ford Model

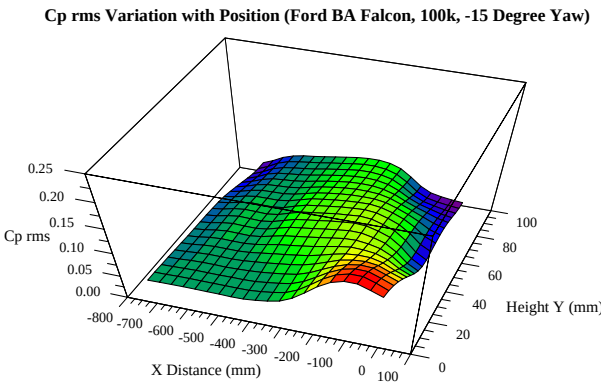

Fig 15. Fluctuating Cp rms Variation, -15º Yaw angles, Ford Model

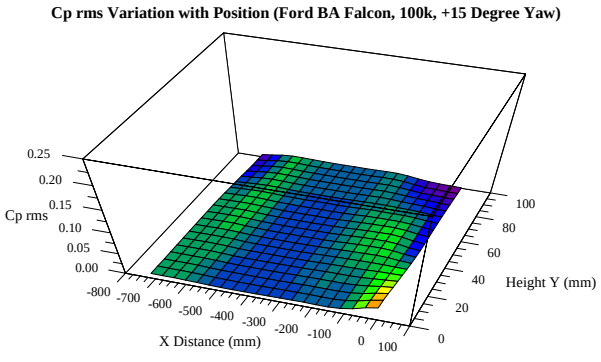

Fig 16. Fluctuating Cp rms Variation, +15º Yaw angles, Ford Model

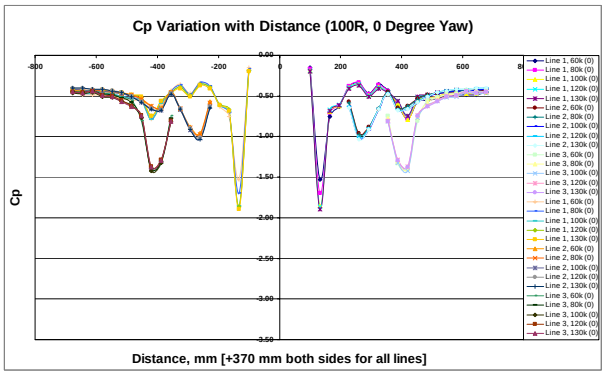

Fig 17. Mean Cp Variation, 0 Yaw angle, 100R Model

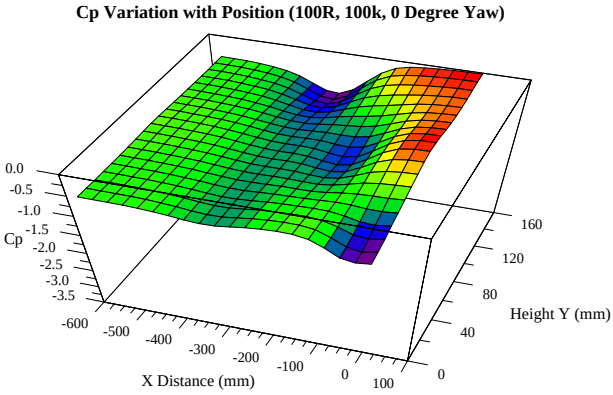

Fig 18. Mean Cp Variation, 0 Yaw angle, 100R Model

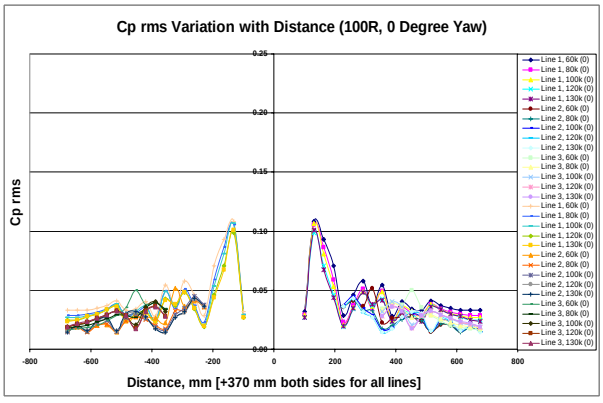

Fig 19. Fluctuating Cp rms Variation, 0 Yaw angle, 100R Model

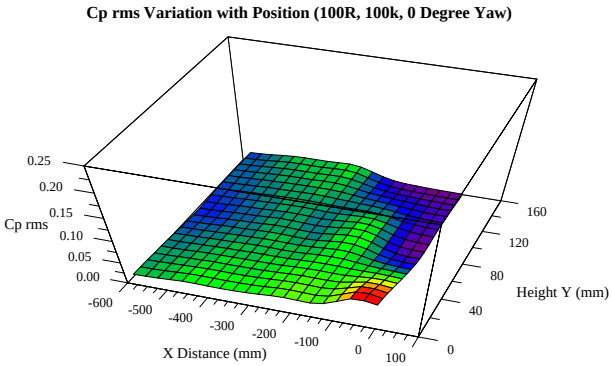

Fig 20. Fluctuating Cp rms Variation, 0 Yaw angle, 100R Model

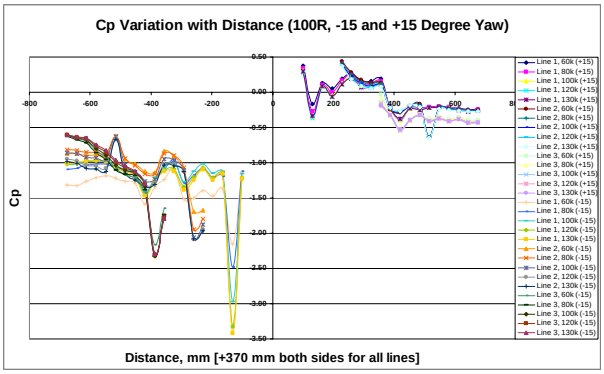

Fig 21. Mean Cp Variation, ±15º Yaw angles, 100R Model

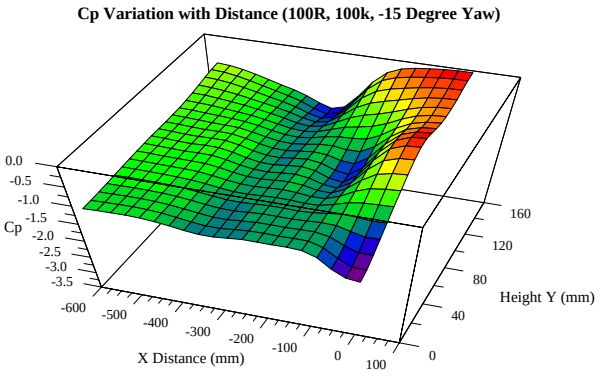

Fig 22. Mean Cp Variation, -15º Yaw angles, 100R Model

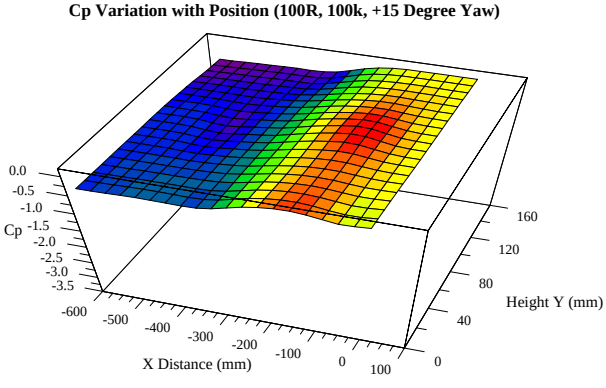

Fig 23. Mean Cp Variation, +15º Yaw angles, 100R Model

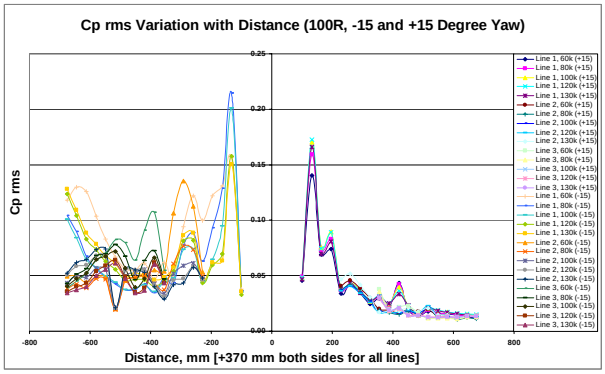

Fig 24. Fluctuating Cp rms Variation, ±15º Yaw angles, 100R Model

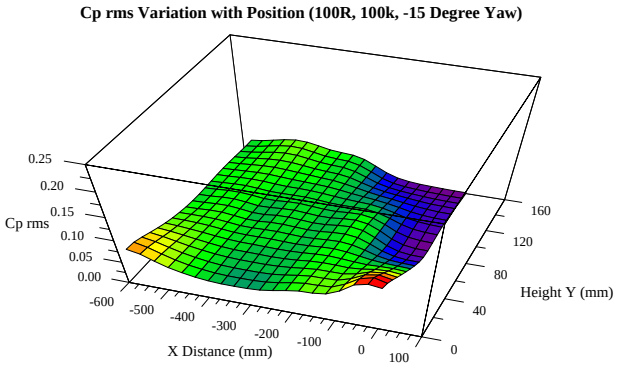

Fig 25. Fluctuating Cp rms Variation, -15º Yaw angles, 100R Model

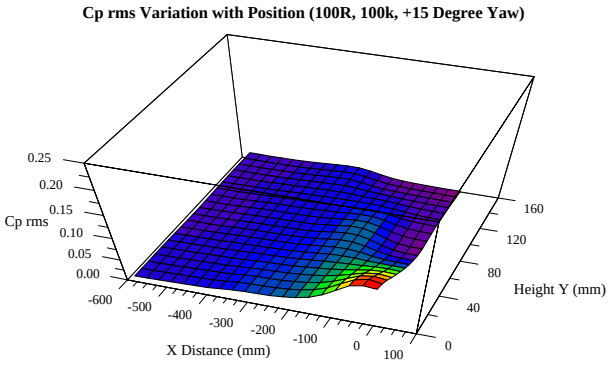

Fig 26. Fluctuating Cp rms Variation, +15º Yaw angles, 100R Model

4. CONCLUSIONS

The following conclusions were made the work presented here:

- The surface mean and fluctuating pressure coefficients are relatively independent of Reynolds numbers at all yaw angles for the Ford model except some minor variations at leeward side yaw angle
- The surface mean and fluctuating pressure coefficients are also relatively independent of Reynolds numbers at all yaw angles for the simplified 100R model except some variations at leeward side yaw angle
- The simplified model generates higher magnitude of pressures compared to the Ford model due to the tighter radius of the A-pillar.
- The leeward side yaw angles generate higher magnitude of fluctuating pressures compared to windward side yaw angles for both models. Therefore, it is expected that the crosswind will have significant effects on aerodynamic noise generation in the A-pillar regions of a car.
- A simplified model can be used to assess the wind noise as the results for the Ford model with correct replica correlate well with the simplified model.

5. ACKNOWLEDGEMENT

The authors would like express their wholehearted gratitude and thanks to Mr George Panagiotakakos and Mr Maumer Smajic for the data acquisition and assistance with the test. Without their assistances, it was not possible to prepare the paper on time.

6. REFERENCES

1. Alam, F., 2000, “The Effects of Car A-pillar and Windshield Geometry on Local Flow and Noise”, Ph.D. Thesis, Department of Mechanical and Manufacturing Engineering, RMIT University, Melbourne, Australia.
2. Alam, F., Zimmer, G. and Watkins, S., 2001, “Surface Pressure Measurements on a Group of Idealised Road Vehicle Models”, *14th Australasian Fluid Mechanics Conference*, 10-14 December, Adelaide, Australia.
3. Haruna, S., Nouzawa, T., Kamimoto, I. and Hiroshi, S., 1990, “An Experimental Analysis and Estimation of Aerodynamic Noise Using a Production Vehicle,” SAE Paper No. 900316, Detroit, USA.
4. Popat, B. C., 1991, “Study of Flow and Noise Generation from Car A-pillars”, Ph.D. Thesis, Department of Aeronautics, Imperial College of Science, Technology and Medicine, The University of London, U.K.
5. Zimmer, G., Alam, F. and Watkins, S. ,2001, “The Contribution of the A-pillar vortex to Passenger Car In-cabin Noise”, *14th Australasian Fluid Mechanics Conference*, 10-14 December, Adelaide, Australia.
6. Zimmer, G. , 2004, “The Contribution of the A-pillar Vortex to Vehicle Interior Noise”, PhD Thesis, Department of Mechanical and Manufacturing Engineering, RMIT University, Melbourne, Australia.